OXFORD

Human Molecular Genetics, 2017, Vol. 26, No. 3 582–598

doi: 10.1093/hmg/ddw418
Advance Access Publication Date: 4 January 2017
Original Article

ORIGINAL ARTICLE

Parkin functionally interacts with PGC-1α to preserve mitochondria and protect dopaminergic neurons

Lu Zheng[1], Nathalie Bernard-Marissal[1], Norman Moullan[2], Davide D'Amico[2], Johan Auwerx[2], Darren J. Moore[1,3], Graham Knott[4], Patrick Aebischer[1] and Bernard L. Schneider[1,*]

[1]Brain Mind Institute, Ecole Polytechnique Fédérale de Lausanne (EPFL), 1015 Lausanne, Switzerland, [2]Laboratory of Integrative and Systems Physiology, EPFL, 1015 Lausanne, Switzerland, [3]Center for Neurodegenerative Science, Van Andel Research Institute, Grand Rapids, MI, 49503, USA and [4]Centre of Interdisciplinary Electron Microscopy, EPFL, 1015 Lausanne, Switzerland

*To whom correspondence should be addressed at: Bernard Schneider, EPFL-SV-BMI-LEN, Station 19, 1015 Lausanne, Switzerland. Tel: +41 21 693 95 05; Fax: +41 21 693 95 20; Email: bernard.schneider@epfl.ch

Abstract

To understand the cause of Parkinson's disease (PD), it is important to determine the functional interactions between factors linked to the disease. Parkin is associated with autosomal recessive early-onset PD, and controls the transcription of PGC-1α, a master regulator of mitochondrial biogenesis. These two factors functionally interact to regulate the turnover and quality of mitochondria, by increasing both mitophagic activity and mitochondria biogenesis. In cortical neurons, co-expressing PGC-1α and Parkin increases the number of mitochondria, enhances maximal respiration, and accelerates the recovery of the mitochondrial membrane potential following mitochondrial uncoupling. PGC-1α enhances Mfn2 transcription, but also leads to increased degradation of the Mfn2 protein, a key ubiquitylation target of Parkin on mitochondria. *In vivo*, Parkin has significant protective effects on the survival and function of nigral dopaminergic neurons in which the chronic expression of PGC-1α is induced. Ultrastructural analysis shows that these two factors together control the density of mitochondria and their interaction with the *endoplasmic reticulum*. These results highlight the combined effects of Parkin and PGC-1α in the maintenance of mitochondrial homeostasis in dopaminergic neurons. These two factors synergistically control the quality and function of mitochondria, which is important for the survival of neurons in Parkinson's disease.

Introduction

Mitochondrial function is crucial for the survival of neurons, a cell type with high-energy demand and which is heavily dependent on oxidative phosphorylation (OXPHOS) for efficient ATP generation. Nigral dopaminergic neurons are constantly exposed to reactive oxygen species produced by dopamine metabolism (1), and these neurons display a large and complex axonal arbor, which raises a major challenge for the trafficking of mitochondria and the supply of energy to their numerous synaptic connections (2). Therefore, nigral dopaminergic neurons are highly dependent on effective mechanisms for the control of the quantity, quality and distribution of mitochondria. Hence, factors that disrupt the homeostasis of mitochondria, such as genetic mutations (3,4) or toxins (4), are often implicated in the progressive degeneration of nigral dopaminergic neurons that characterizes Parkinson's disease (PD).

In particular, mutations leading to the loss of Parkin function account for the most common familial forms of PD with autosomal recessive inheritance (5,6). In addition, sporadic PD is

Received: August 13, 2016. **Revised:** December 1, 2016. **Accepted:** December 2, 2016

also associated with a decrease of Parkin activity (7). The Parkin protein, which functions as an E3 ubiquitin ligase, plays a key role in the quality control of mitochondria via the regulation of mitophagy (8,9). The pathway regulating mitophagy is controlled by PINK1-mediated phosphorylation of Parkin and ubiquitin moieties, via a feed-forward mechanism leading to the ubiquitylation of mitochondrial proteins (10–12). Among several targets, the poly-ubiquitination of PINK1-phosphorylated Mitofusin 2 (Mfn2) protein by Parkin contributes to the autophagic clearance of damaged mitochondria (13,14). However, Parkin-mediated mitophagy is most evident in immortalized cell lines exposed to uncoupling agents. Parkin translocation and mitophagy is observed only at a low rate in neuronal cells (15,16), which have a distinct metabolic profile from immortalized cell lines. Therefore, it is critical to explore the mechanisms that tightly control mitochondrial turnover in neurons.

In addition to the induction of mitophagy, Parkin has a multi-faceted role in controlling the function of mitochondria. Indeed, mitochondria exposed to stress can operate various mechanisms to preserve their homeostasis, such as organelle fusion/fission, and protein quality control systems including the generation of mitochondria-derived vesicles (MDV) and unfolded protein response (17,18). Parkin regulates key proteins involved in mitochondrial dynamics (19), transport (20) and function (21), either through non-degradative ubiquitination, or by promoting their proteasomal degradation (22). In particular, Parkin has been shown to degrade the repressor PARIS, thereby promoting the transcription of *PPARGC1A*, a master regulator of mitochondrial biogenesis (23). It has been proposed that the concerted action of Parkin and PGC-1α may have an important role by controlling the turnover of a functional pool of mitochondria (24,25), or more directly, by promoting mitochondrial repair (26–28). Remarkably, a meta-analysis of gene expression in laser-captured dopamine neurons and *substantia nigra* (SN) has highlighted the down-regulation of PGC-1α activity in sporadic PD patients (29), which prompts the clinical evaluation of disease-modifying treatments enhancing PGC-1α activity (30).

Parkin and PGC-1α are two key proteins participating in the regulation of mitochondria homeostasis. Hence, understanding the interplay between these two factors is important to unveil the mechanisms that govern mitochondrial turnover in the context of PD. Here, we hypothesized that Parkin and PGC-1α may have combined effects on maintaining mitochondrial function. These effects were explored both in primary neuronal cell cultures, as well as in dopaminergic neurons *in vivo*. We observed that the cooperation of Parkin and PGC-1α increases mitochondrial density in cortical neurons. By maintaining a robust respiratory profile, these factors effectively rescue mitochondria from the loss of the membrane potential. In conditions where PGC-1α is continuously overexpressed in the rat SN, the activity of Parkin controls the survival of dopaminergic neurons and mitochondrial homeostasis, revealing the negative effects of the disease-associated Parkin mutants (25).

Results

Overexpression of Parkin upregulates the transcription of PGC-1α

We first determined the effect of Parkin on the transcription of *Ppargc1a* in primary neurons derived from the mouse cortex. The amplicon used for quantification of *Ppargc1a* mRNA spans exons 10 and 11, a region which is present in most *Ppargc1a* splicing isoforms, including the previously described brain-specific isoforms (31), but not in the N-terminal truncated isoforms (NT-PGC-1α). *Ppargc1a* mRNA level was significantly increased in primary neurons overexpressing human wild-type Parkin (Supplementary Material, Fig. S1A). In neurons derived from Parkin-null mice, the basal expression of *Ppargc1a* was significantly reduced, which further confirmed a role of Parkin in regulating *Ppargc1a* expression. Parkin overexpression significantly rescued *Ppargc1a* mRNA level, whereas the K161N and R42P Parkin mutants associated with early-onset recessive PD had no significant effect (Supplementary Material, Fig. S1A). Conversely, we examined whether PGC-1α overexpression induced any change in the transcription of PD-associated genes, and found no significant differences in the expression of *Snca, Pink1, Park7 or Lrrk2* (Supplementary Material, Fig. S1B). *Park2* mRNA level was on average 38% reduced when PGC-1α was overexpressed, which was statistically not significant ($P = 0.09$). Overall, these results confirmed that Parkin induces the expression of the transcriptional co-activator PGC-1α. Therefore, we next sought to explore the effects of these two factors on mitochondrial biogenesis.

Co-expression of Parkin and PGC-1α enhances both mitochondrial biogenesis and mitophagic activity

To assess the effects of Parkin and PGC-1α on the number of mitochondria, primary cortical neurons were transduced with AAV2/6 vectors encoding either Parkin or PGC-1α, or with a combination of these two vectors. Total vector doses were kept constant by adding the necessary amount of a non-coding control vector. Seven days post-infection, the relative numbers of mitochondrial DNA (mtDNA) copies per cell were determined by real-time PCR, measuring the abundance of a mitochondrial gene (*Mt-Co2 or 16S*) with respect to a nuclear gene (*Ucp2 or Hk2*) (Fig. 1A). Relative mtDNA copy numbers were significantly increased in neurons overexpressing either PGC-1α or Parkin. And most remarkably, when these two proteins were co-overexpressed, the relative abundance of mtDNA was significantly further increased compared to all the other conditions. To obtain additional evidence for increased mitochondrial biogenesis, we infected neurons with a viral vector encoding the mitochondrial fluorescent reporter MitoDsRed. Transduced neurons were analysed by flow cytometry to determine the mean red fluorescence intensity as an indicator of total mitochondrial mass per cell (Fig. 1B). Average MitoDsRed intensity was significantly increased in cortical neurons overexpressing either PGC-1α or Parkin. Again, the MitoDsRed intensity further increased when these two factors were co-expressed, confirming the combined effect of Parkin and PGC-1α on the density of mitochondria.

Next, we verified that mitochondrial biogenesis observed in neurons co-expressing PGC-1α and Parkin was not simply due to the increased transcriptional activity of PGC-1α in the presence of Parkin. To that end, mitochondrial biogenesis was evaluated in PGC-1α-null neurons. Neither the expression of Parkin, nor PGC-1α alone had an effect on mtDNA copies per cell (Fig. 1C). Only when both factors were co-expressed, we observed an increase in mtDNA copy number. These findings demonstrate that Parkin has an effect on mitochondrial biogenesis only in the presence of PGC-1α. In Parkin-null neurons however, Parkin and/or PGC-1α had clear effects on mtDNA abundance, which is similar to wild-type neurons (Fig. 1D). Together, these results show that PGC-1α is the key factor driving mitochondrial biogenesis under these experimental conditions, and that Parkin and PGC-1α have synergistic effects on the abundance of mitochondria.

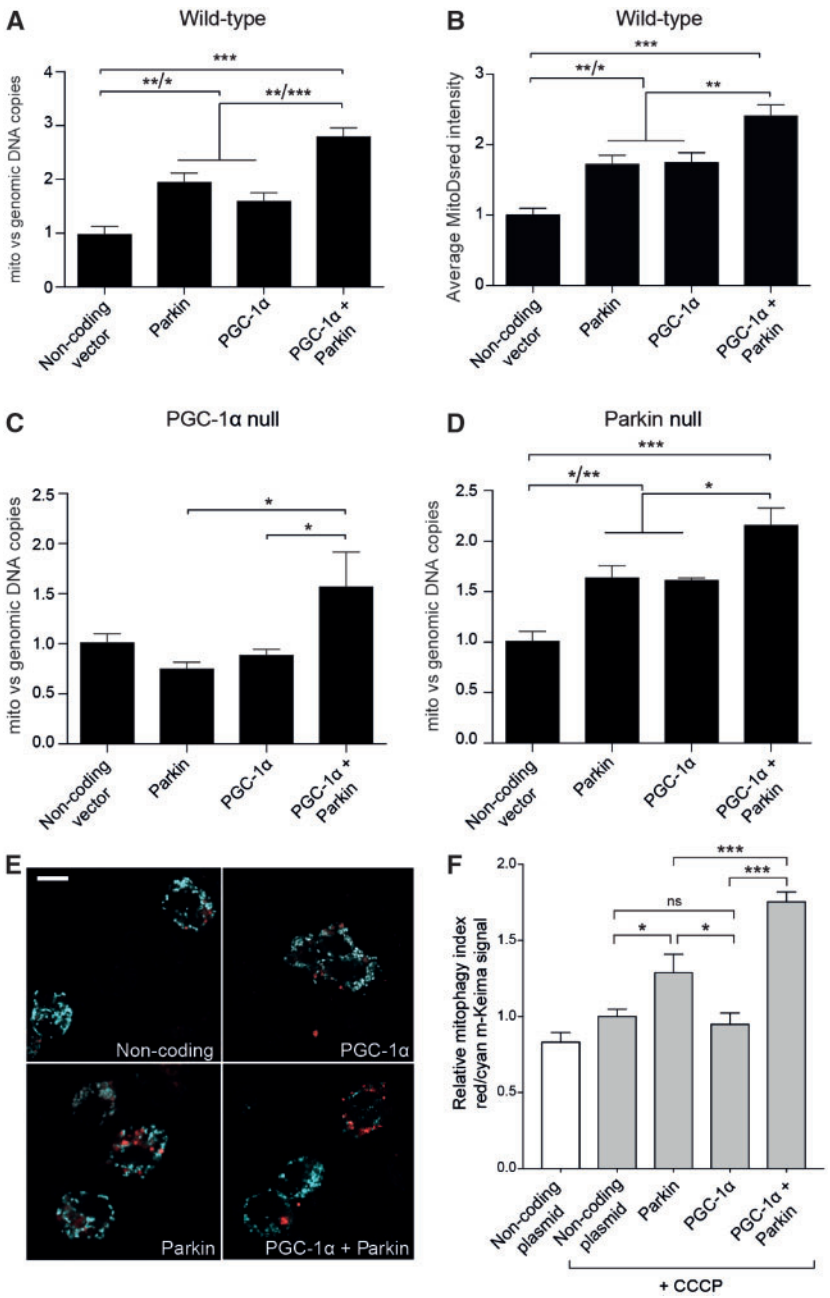

Figure 1. PGC-1α and Parkin cooperatively control mitochondrial biogenesis and mitophagic activity. Primary cortical neurons were transduced either with a non-coding AAV2/6 vector (control), a Parkin-expressing vector, a PGC-1α-expressing vector, or a combination of both. Real-time PCR was used to quantify mtDNA (*Mt-co2, 16S*) copies normalized to cell genomic DNA (*Ucp2, Hk2*) copies in (**A**) wild-type cortical neurons ($n = 4$–8), (**C**) PGC-1α-null neurons ($n = 3$) and (**D**) Parkin-null neurons ($n = 3$). (**B**) Mean MitoDsRed intensity per cell was measured by flow cytometry in cortical neurons co-infected with an AAV-MitoDsRed vector ($n = 4$–8). Data are normalized to the control condition transduced with the non-coding AAV2/6 vector, and represented as mean ± SEM. (**E**,**F**) Detection and quantitation of mitophagy using the mitochondria-targeted m-Keima probe. (**E**) Representative images of SH-SY5Y cells co-transfected with m-Keima and with the non-coding, PGC-1α and Parkin constructs. To induce mitophagy, the cells are treated with 20 μM CCCP for 16 h. Scale bar: 10 μm. Red signal corresponds to the excitation of the ionized form of m-Keima in regions where mitophagy is on going. In cyan, non-ionized m-Keima signal is shown and represents mitochondria at pH 7. (**F**) The mitophagy index is measured by calculating the red/cyan ratio of the fluorescence intensity signal (number of replicates: 7–9 per condition, representing a total of 20–30 cells). A control condition with SH-SY5Y cells co-transfected with non-coding and m-Keima plasmids, and not exposed to CCCP, is shown for comparison. Statistical analysis for A, B and D: one-way ANOVA, followed by Newman-Keuls multiple comparison post-hoc test: $^{*}P < 0.05$, $^{**}P < 0.01$, $^{***}P < 0.001$. For C: one-way ANOVA with $F(3,8)=3.721$, followed by unrestricted Fisher's LSD multiple comparison post-hoc test: $^{*}P < 0.05$. For F: two-way ANOVA (all conditions except control without CCCP) with $F(3,28)=10.561$ (PGC-1α x Parkin interaction), followed by Newman-Keuls multiple comparison post-hoc test: ns non-significant, $^{*}P < 0.05$, $^{***}P < 0.001$. Data represent mean ± SEM.

The number of mitochondria is controlled by both the biogenesis and mitophagic degradation of mitochondria. Using SH-SY5Y neuroblastoma cells, we determined the effect of co-expressing Parkin and PGC-1α on the rate of mitophagy. Cells were exposed to CCCP for 16 h to promote mitophagy, which was measured by co-expressing the mitochondria-targeted m-Keima, a pH-sensitive fluorescent reporter resistant to lysosomal proteases (Fig. 1E) (32). In contrast to PGC-1α, which alone

did not have any effect on mitophagic activity, overexpressing human Parkin increased mitophagy in SH-SY5Y cells exposed to CCCP (Fig. 1F). Remarkably, the proportion of mitochondria present in the lysosomal compartment was higher in cells co-expressing Parkin and PGC-1α than in the Parkin alone condition (Fig. 1F). This result indicates that Parkin and PGC-1α have combined effects both on the biogenesis and mitophagic degradation of mitochondria. In cortical neurons, Parkin and PGC-1α together maintain an abundant pool of mitochondria.

Parkin increases the maximal respiratory capacity of cortical neurons when PGC-1α is co-expressed

As the number of mitochondria increases following co-expression of PGC-1α and Parkin, it is important to determine the overall effect of these factors on mitochondrial metabolism. To this end, we measured the oxygen consumption rate (OCR), which is an important indicator of OXPHOS activity and mitochondrial function. The respiration of cortical neurons was measured under basal conditions as well as upon treatment with CCCP, a protonophore leading to mitochondrial uncoupling. Furthermore, to measure residual OCR in the absence of ATP production, separate wells were treated with oligomycin, an inhibitor of ATPase activity.

Similar to the previous experiment, cortical neurons were infected seven days before analysis with viral vectors that were either non-coding, encoding Parkin, or encoding PGC-1α. Expectedly, we observed that PGC-1α overexpression significantly increased basal OCR compared to control cells (Fig. 2A and B). Neuronal respiration was further enhanced upon CCCP exposure. However, the maximal OCR of PGC-1α-expressing neurons in the presence of CCCP was only transiently increased, and the average respiration measured over 21 min of CCCP exposure was not significantly different compared to control (Fig. 2A and D). In cortical neurons co-expressing Parkin and PGC-1α, basal OCR was very similar to PGC-1α alone (Fig. 2A and B). However, upon CCCP treatment, we observed a robust and more sustained increase in OCR (Fig. 2A). The maximal OCR was significantly increased compared to neurons transduced either with the non-coding vector, or with AAV-PGC-1α (Fig. 2D). The reserve respiratory capacity, which represents the percentage increase in OCR with respect to basal OCR, was dramatically enhanced only when PGC-1α and Parkin were co-expressed (Fig. 2C). Measurement of OCR in the presence of oligomycin showed that there was no difference in the respiration dedicated to ATP production (% decrease in OCR), indicating that the coupling of mitochondrial respiration to the electron transport chain remained very similar across all three conditions (Fig. 2C).

Next, we tested if the loss of Parkin activity caused by PD mutations suppresses the synergistic effect of Parkin and PGC-1α on the mitochondrial respiratory capacity. Variants of human Parkin carrying the R42P mutation (defective in ubiquitin ligase activity) or the K161N mutation (defective in mitophagy) were co-expressed with PGC-1α. In contrast to wild-type Parkin, the two recessive PD-associated Parkin mutants failed to significantly increase the maximal respiratory capacity in primary cortical neurons (Fig. 2E). The R42P mutant even further compromised mitochondrial activity. These results show that Parkin activity, combined with the expression of PGC-1α, enhances the mitochondrial respiratory capacity in neurons.

To determine if the effect of Parkin on CCCP-induced respiration is indeed potentiated by PGC-1α, we conducted a similar experiment to measure the effect of Parkin alone on mitochondrial respiration. Parkin overexpression did not induce any major change in basal OCR (Fig. 2F and G). Remarkably, we found that in the absence of PGC-1α overexpression, Parkin instead reduced the maximal OCR (Fig. 2F and H), consistent with a significant decrease in the respiratory reserve capacity (Fig. 2I). Therefore, it appears that PGC-1α activity is critical for Parkin to increase the mitochondrial respiratory capacity and maintain a resilient pool of neuronal mitochondria, which exhibit robust metabolic activity under uncoupling stress.

Co-expression of PGC-1α and Parkin preserves the mitochondrial membrane potential

Cellular respiration is critical to maintain the mitochondrial membrane potential (Δψm) via the electron transport chain (ETC) activity. To determine if PGC-1α and Parkin affect Δψm, we labelled primary cortical neurons with JC-1, a Δψm-sensitive dye that aggregates in polarized mitochondria and shifts its emission maximum from 525 nm (green) to 590 nm (red). Neurons were exposed to CCCP for 20 min, and then maintained in medium without CCCP. Although the ratio of green/red JC-1 fluorescence cannot be used to detect small variations in Δψm, red signal is an indicator of the presence of mitochondria which have recovered Δψm. We used JC-1 to assess Δψm recovery approximately 30 min after CCCP removal. As expected, the green/red ratio was increased in control neurons following CCCP exposure (Fig. 3A). Overexpression of either PGC-1α or Parkin alone only marginally enhanced Δψm recovery. In contrast, the co-expression of Parkin and PGC-1α had a robust effect on recovery of Δψm, and the ratio of green/red JC-1 fluorescence was similar to the level seen in neurons not exposed to CCCP (Fig. 3A). When PGC-1α was co-expressed with either the R42P or the K161N Parkin mutant, Δψm did not significantly recover, highlighting the need for intact Parkin function. These results demonstrate that the increase in maximal respiration observed in neurons co-expressing Parkin and PGC-1α enhances their ability to regain Δψm following CCCP exposure.

Loss of Δψm is coupled with ROS production, which can impair the replication and integrity of mtDNA (33,34). Therefore, we sought to determine the effect of Parkin and/or PGC-1α expression in cortical neurons following longer exposure to CCCP. Neurons were exposed to 20 μM CCCP for 24 h, six days after transduction with AAV vectors. Real-time PCR was used to determine the amount of mtDNA (*Mt-co2, 16S*), relative to cellular gDNA (*Ucp2, Hk2*) (Fig. 3B). Only the co-expression of Parkin and PGC-1α resulted in higher mtDNA copy numbers compared to neurons transduced with the non-coding vector. Neither the expression Parkin or PGC-1α had a significant effect on mtDNA copy numbers.

PGC-1α and Parkin promote transcription of mitochondrial genes in cortical neurons

To explore how Parkin and PGC-1α co-regulate mitochondrial respiration and function, we next assessed by real-time PCR changes in the expression of several genes related to mitochondrial function, and that are transcriptionally controlled by PGC-1α (23,35,36). Transcriptional changes were measured in primary cortical neurons, seven days after transduction with AAV2/6 vectors encoding Parkin, PGC-1α, or a combination of these two vectors (Fig. 4). Expectedly, several mitochondrial genes showed robust transcriptional changes in PGC-1α-overexpressing neurons. Genes showing significantly higher mRNA levels included *Tfam*, *Atp5g1*, *Ndufs1*, *Cox4*, *Mfn1*, *Mfn2*, *Vdac1*

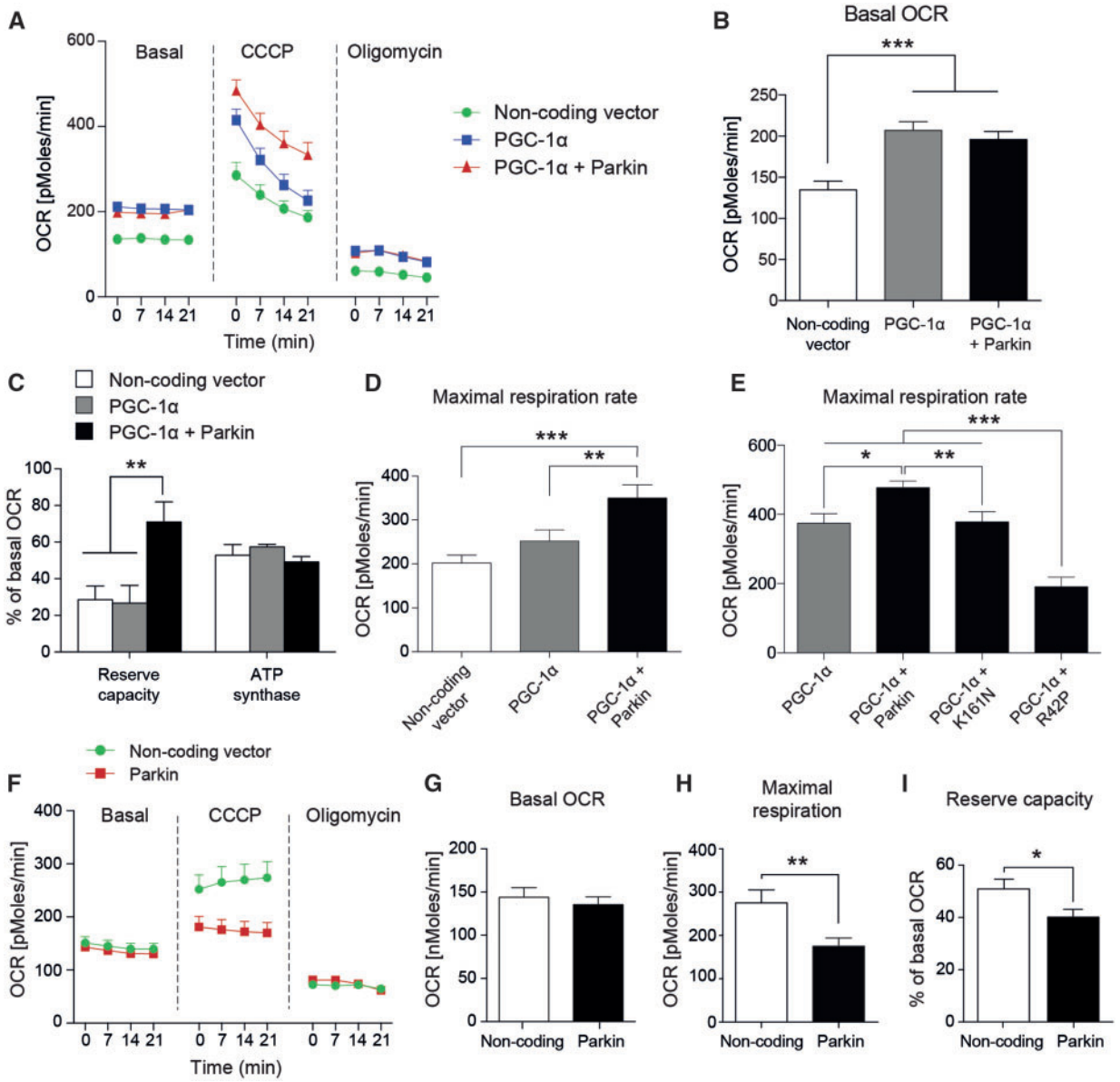

Figure 2. Parkin, but not the PD-associated Parkin mutants, cooperates with PGC-1α to enhance maximal respiration rate in neurons. **(A)** Profile of the oxygen consumption rate (OCR) measured in cortical neurons transduced with PGC-1α and Parkin vectors. Measurements at four different time points were collected for basal respiration, maximal respiration (10 μM CCCP), and during the inhibition of ATP synthase (5 μM oligomycin). **(B)** Quantification of the average basal OCR ($n = 26–28$). **(C)** Quantification of the reserve respiratory capacity ($n = 13–14$) and coupling efficiency (% of basal OCR used for ATP synthase activity; $n = 12–14$), expressed as the average over all four measurements. **(D)** Maximal OCR ($n = 13–14$). **(E)** Maximal OCR (average of four measurements) in PGC-1α overexpressing neurons, comparing the effect of Parkin and the PD-associated mutants ($n = 15$). **(B-E)** One-way ANOVA, Newman-Keuls multiple comparison post-hoc test. **(F)** OCR profile of cortical neurons transduced with the control non-coding or the Parkin-expressing vector. **(G-I)** Basal OCR ($n = 26–28$), maximal OCR ($n = 12–17$) and reserve respiratory capacity ($n = 12–17$). Two-tailed unpaired Student's *t*-test. All data represent mean ± SEM. $^{*}P < 0.05$, $^{**}P < 0.01$.

and *Clpp*, whereas the expression of *Rhot1* remained unchanged. The overexpression of Parkin alone also significantly increased the transcription of the same genes, which is consistent with the increase of PGC-1α activity observed in this condition (Supplementary Material, Fig. S1). For most of the upregulated genes, mRNA levels were very similar under conditions where either PGC-1α alone or PGC-1α together with Parkin was overexpressed. Nonetheless, compared to both the control and PGC-1α conditions, Parkin co-expression further increased the level of the mRNAs encoding *Tfam* and *Ndufs1*. *Tfam* is a mitochondrial transcription factor crucially implicated in the amplification of mtDNA and mitochondrial biogenesis. *Ndufs1* is a key subunit of complex I, which transfers electrons from NADH to the respiratory chain and initiates OXPHOS. Therefore, the synergistic effect of Parkin and PGC-1α on the expression of *Tfam* and *Ndufs1* is likely to contribute to the observed increase in the maximal respiration rate of cortical neurons co-expressing both factors.

However, Parkin does not appear to be a strong enhancer of the transcriptional activity of PGC-1α. Therefore, we sought to explore other possible mechanisms that may explain the robust synergistic effect between Parkin and PGC-1α on mitochondrial homeostasis (Figs 2 and 3). To this end, we measured if PGC-1α had any effect on the abundance of mitochondrial proteins, in particular those that are known substrates of Parkin-mediated ubiquitylation.

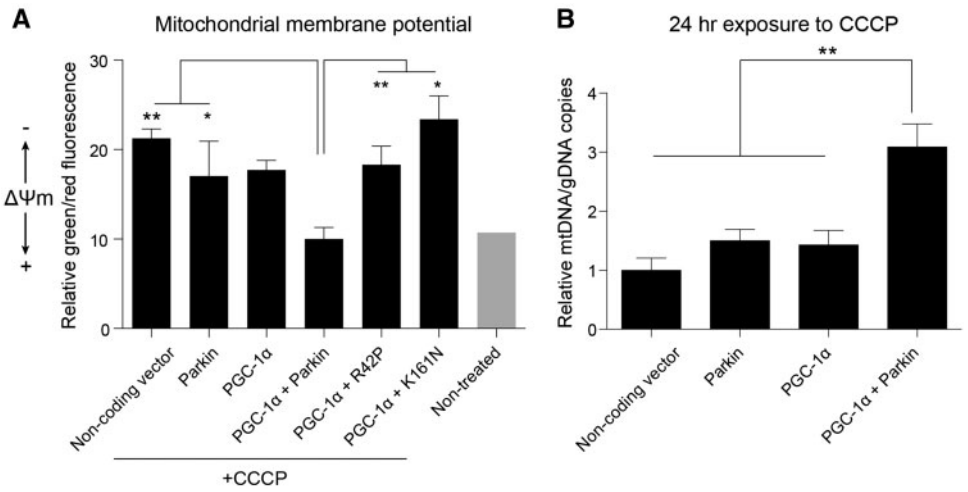

Figure 3. Parkin, but not its PD-associated mutants, cooperates with PGC-1α to maintain mitochondrial membrane potential. (**A**) Mitochondrial membrane potential (Δψm) in cortical neurons transduced with AAV-PGC-1α and AAV-Parkin vectors. Δψm was measured using the JC-1 dye, 20 min after removal of 10 μM CCCP ($n = 3$ for all CCCP-exposed conditions, except $n = 2$ for the control; the value of a well not treated with CCCP is shown for indication). Data represent mean ± SEM. One-way ANOVA, Fischer's LSD post-hoc test. $^{*}P < 0.05$, $^{**}P < 0.01$. (**B**) mtDNA integrity after 24 h of CCCP treatment (10 μM). Real-time PCR was used to quantify mtDNA copies (mean value of *Mt-co2*, *16S*) normalized to cell genomic DNA copies (mean value of *Ucp2* and *Hk2*) ($n = 4$–8). Data represent mean ± SEM. One-way ANOVA, Newman-Keuls multiple comparison post-hoc test. $^{**}P < 0.01$.

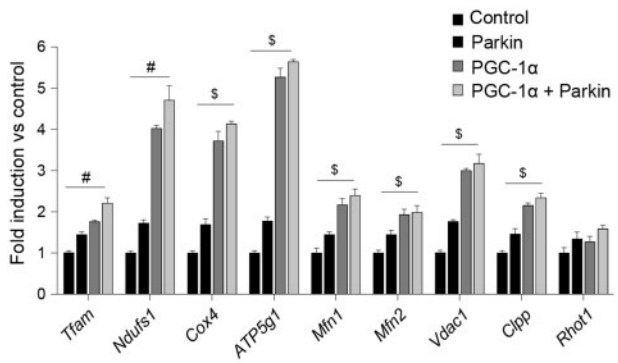

Figure 4. Mitochondrial genes are upregulated by the overexpression of PGC-1α and Parkin. mRNA levels of selected genes controlled by PGC-1α were measured by real-time PCR following overexpression of PGC-1α and/or Parkin. For each gene, mRNA expression levels (relative to 36B4, internal control) were normalized to those in the control neurons transduced with a non-coding vector, and expressed as arbitrary values ($n = 3$). One-way ANOVA, Newman-Keuls multiple comparison post-hoc test. Hashtag symbol (#) indicates a significant difference ($P < 0.05$) between any pair of conditions; Dollar sign ($) indicates a significant difference ($P < 0.05$) between any pair of conditions, except PGC-1α versus PGC-1α+Parkin.

PGC-1α controls the abundance of mitofusin 2, a substrate of Parkin

As Parkin primarily exerts E3 ubiquitin ligase activity, we next sought to determine if Parkin overexpression increases the ubiquitination of PGC-1α. SH-SY5Y neuroblastoma cells were transfected with plasmids encoding Parkin, EGFP-PGC-1α and ubiquitin, and the overexpressed EGFP-PGC-1α was immunoprecipitated to determine the ubiquitination level. Parkin overexpression did not increase levels of ubiquitinated PGC-1α, suggesting that PGC-1α is unlikely to be a substrate of Parkin (Supplementary Material, Fig. S2).

Next, we examined if PGC-1α controls the ubiquitination and degradation of Parkin substrates known to affect mitochondrial function. Parkin has been shown to control mitochondrial homeostasis via the ubiquitylation of proteins that are mainly present on the outer mitochondrial membrane (37). Mitofusin 1 (Mfn1), Mfn2 and Voltage-Dependent Anion Channel 1 (VDAC1) are three substrates of Parkin that serve important roles in the function and turnover of mitochondria (14,38,39). In order to assess the modification and degradation of these proteins independently of the effect of PGC-1α on the transcription of the corresponding endogenous genes, we used SH-SY5Y neuroblastoma cells transfected with a plasmid expressing either Mfn1, Mfn2 or VDAC1. Co-transfections were performed to determine the effect of Parkin and/or PGC-1α on the level and ubiquitination of the overexpressed tagged proteins. Parkin indeed induced the ubiquitination of Mfn1 in SH-SY5Y cells, but PGC-1α had no effect on the level of ubiquitinated Mfn1 (Fig. 5A). VDAC1 also showed increased ubiquitination following Parkin expression. However, there was also no change in the overall level of VDAC1 in any of the conditions, and PGC-1α had no effect on the level of ubiquitinated VDAC1 (Fig. 5B). Whereas PGC-1α did not influence the overall protein levels of Mfn1 and VDAC1, PGC-1α overexpression significantly reduced Mfn2 level in SH-SY5Y cells (Fig. 5C and D). This effect was particularly evident in the absence of Parkin (Fig. 5C and D). To determine which pathway was involved in Mfn2 degradation, we performed a similar experiment in the presence of either a protease inhibitor (MG-132) or an autophagy inhibitor (3-methyladenine, 3-MA). MG-132 prevented the reduction of Mfn2 levels seen in cells overexpressing PGC-1α (Fig. 5C and D). Therefore, Mfn2 degradation was likely mediated by the ubiquitin/proteasome system and/or calpain (40), which are both blocked by MG-132. In SH-SY5Y cells treated with 3-MA, PGC-1α decreased Mfn2 levels to a similar extent as in untreated cells. In the presence of 3-MA, the effect of PGC-1α on Mfn2 was also significant in cells overexpressing Parkin. Together, these findings demonstrate that PGC-1α overexpression can induce the degradation of Mfn2 via mechanisms that are largely independent of Parkin and do not involve autophagy. As Mfn2 is the substrate of the mitochondrial E3 ubiquitin protein ligase 1 (MUL1), we analysed the expression of

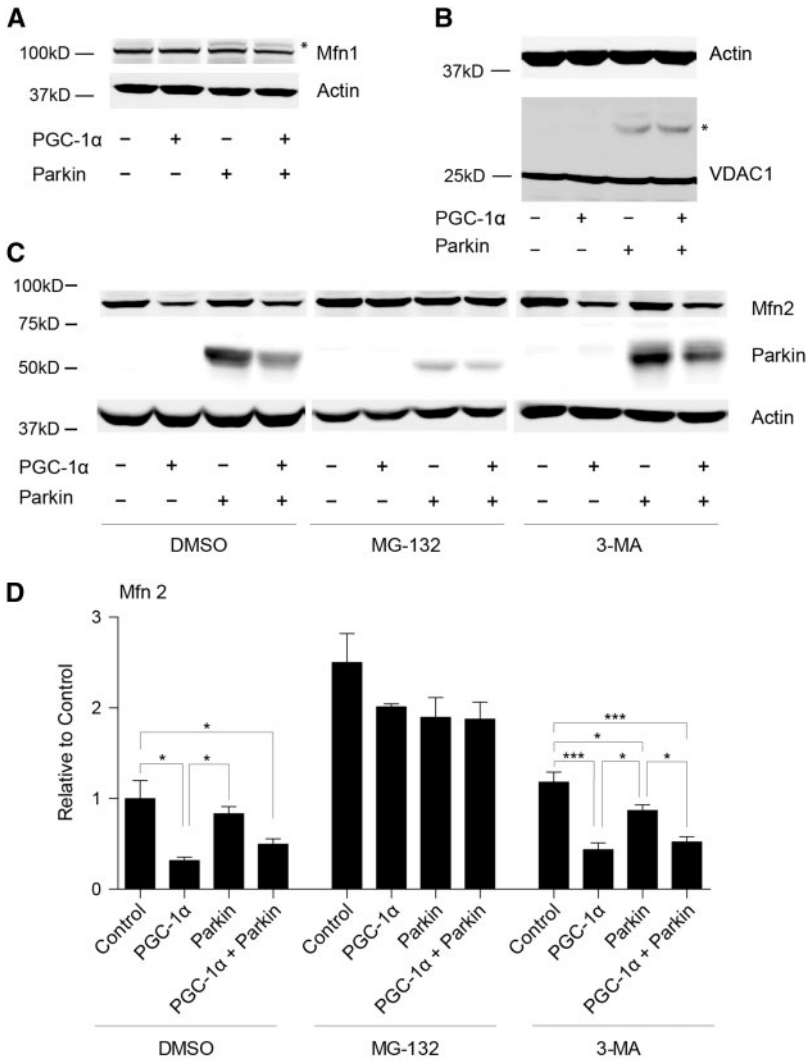

Figure 5. PGC-1α induces the degradation of the Parkin substrate Mitofusin 2. SH-SY5Y neuroblastoma cells were transfected with plasmids encoding EGFP-PGC-1α and/or Parkin, and plasmids encoding the Parkin substrates Mfn1, VDAC1 and Mfn2. (**A**) Western blot showing the levels of Mfn1 in each condition. Actin is used as a loading control. Note the presence of ubiquitinated Mfn1 (*) in the cells expressing Parkin. (**B**) Western blot showing the levels of VDAC1 in each condition. Note the presence of ubiquitinated VDAC1 (*) in the cells expressing Parkin. (**C**) Western blot showing the levels of Mfn2 in each condition. In parallel transfections, cells were treated for 15 h with either the proteasome inhibitor MG-132 or the autophagy inhibitor 3-MA. The expression of Mfn2, Parkin and actin were revealed for each condition. (**D**) Quantification of Mfn2 levels relative to actin in three independent western blots. Data normalized to the DMSO control condition are expressed as mean ± SEM, $^{*}P < 0.05$, $^{***}P < 0.001$. One-way ANOVA, Newman-Keuls multiple comparison post-hoc test.

MUL1 in cells with increased PGC-1α activity. The protein levels of MUL1 were indeed increased in SH-SY5Y cells overexpressing PGC-1α (Supplementary Material, Fig. S4). Similarly, *Mul1* mRNA levels were found to be higher in mouse cortical neurons overexpressing PGC-1α. PGC-1α may therefore modify the effects of Parkin on mitochondria by enhancing the turnover of the Parkin substrate Mfn2.

Parkin controls the survival of nigral dopaminergic neurons overexpressing PGC-1α and decreases amphetamine-induced rotational behaviour

Overexpression of PGC-1α modifies Parkin effects in cortical neurons by enhancing the biogenesis and the homeostasis of mitochondria. Next, we sought to explore the effect of Parkin and PGC-1α on dopaminergic neurons in the rat SN. Indeed, nigral dopaminergic neurons may critically depend on mitochondrial function to support their high metabolic demand (41,42). In addition, dopamine metabolism may cause oxidative stress and thereby compromise the mitochondrial function. Therefore, it is important to determine how Parkin and PGC-1α affect mitochondria quantity and quality in dopaminergic neurons *in vivo*. Despite the undisputed role of Parkin in familial PD, it has been notoriously difficult to assess its pathological effects in rodents. We explored the effects of Parkin in dopaminergic neurons overexpressing PGC-1α to induce mitochondrial biogenesis. Indeed, the chronic overexpression of PGC-1α leads to the selective loss of dopaminergic markers and neuronal degeneration in the rat SN and these effects may be in part caused by a failure of mitochondrial quality control (43).

To determine if Parkin can rescue the PGC-1α-induced deficits observed in dopaminergic neurons *in vivo*, we co-expressed PGC-1α with either wild-type Parkin, or two of its mutated forms (R42P and K161N), using stereotaxic injections of AAV vectors. Co-injection of AAV-PGC-1α together with a non-coding vector

was used for reference. The survival and function of nigral dopaminergic neurons was assessed at four months post-injection. Nissl staining was used to determine in the SN *pars compacta* the total number of neurons with a morphology similar to dopaminergic neurons (Fig. 6B and Supplementary Material, Fig. S4A). In addition, VMAT2 was used as a marker to determine the number of nigral dopaminergic neurons (Fig. 6C and Supplementary Material, Fig. S4B). The overexpression of PGC-1α led to a progressive loss of nigral neurons in the injected SN (59 ± 5% loss of Nissl$^+$ neurons; 67 ± 6% loss of VMAT2$^+$ cell bodies), compared to the contralateral hemisphere (Fig. 6A–C). In the *striatum*, the axonal immunoreactivity for tyrosine hydroxylase (TH) was decreased by 51 ± 7% (Fig. 6A and D). Co-expression of wild-type human Parkin had a significant protective effect, decreasing the loss of Nissl$^+$ neurons in the injected SN *pars compacta* to 43 ± 5% (Fig. 6A and B). When measuring the number of VMAT2-positive neurons and striatal TH immunoreactivity, the Parkin group also showed a trend towards neuroprotection compared to the co-injection of a non-coding vector (Fig. 6C and D). The fact that it did not reach significance might indicate that Parkin had only a partial rescue effect on the dopaminergic markers.

In contrast to wild-type Parkin, the co-expression of the K161N or R42P Parkin mutants did not show any protective effect against the degeneration induced by overexpression of PGC-1α. In the SN *pars compacta*, the loss of VMAT2$^+$ and Nissl$^+$ neurons in the groups expressing mutated Parkin reached values that were very similar to the co-injection of control non-coding vector, and significantly different from wild-type Parkin (Fig. 6A and C). In the *striatum*, the decrease in TH immunoreactivity caused by the expression of PGC-1α was further exacerbated by the co-expression of either K161N (71 ± 7%) or R42P Parkin (75 ± 7%), as compared to the non-coding vector (51 ± 7%). These results suggest a possible negative effect of mutant Parkin on the preservation of the dopaminergic innervation, which is significantly different from wild-type Parkin (Fig. 6A and D).

To evaluate the effects of Parkin on the dopaminergic function, we assessed amphetamine-induced rotations that reflect the motor asymmetry caused by dopamine release following amphetamine exposure. As previously shown (43), the chronic overexpression of PGC-1α led to motor asymmetry, with contraversive rotations reaching 3.54 ± 1.02 turns/min at month 2, and 3.05 ± 0.96 turns/min at month 4 after vector injection (Supplementary Material, Fig. S5A and B). Two months after injection, wild-type Parkin significantly rescued motor asymmetry (1.36 ± 0.41 turns/min). In contrast, the K161N and R42P mutants had no effect on the rotational behaviour caused by unilateral injection of the PGC-1α vector (Supplementary Material, Fig. S5B). At 4 months post-injection, the difference between the group expressing PGC-1α, and the group expressing PGC-1α and Parkin was no longer significant, suggesting that Parkin-mediated effects on the motor function were transient in nature. This phenomenon might be due to a progressing neurodegeneration caused by PGC-1α overexpression.

Next, we assessed the effect of Parkin and mutants in the absence of PGC-1α. AAV vectors expressing wild-type Parkin, the K161N mutant and the R42P mutant were injected in the rat SN, using the same dose as in the previous experiment. Four months post-injection, we observed that Parkin mutants were expressed at lower levels compared to wild-type Parkin (Fig. 6E), as previously reported for the R42P mutant (44). Most importantly, both in the animals expressing Parkin and its mutated variants, there was neither a loss of neurons expressing TH in the SN *pars compacta*, nor a decrease of TH immunoreactivity in the *striatum*. Hence, only when nigral neurons in the adult SN overexpressed PGC-1α, did their survival depend on the induced expression of Parkin, revealing the lack of protective effect of the Parkin mutations under these conditions. Together, these findings support the hypothesis that Parkin activity can modify the survival of nigral neurons and the expression of dopaminergic markers *in vivo*, at least under conditions where PGC-1α is overexpressed.

Parkin and PGC-1α control the density and morphology of mitochondria in nigral dopaminergic neurons

To investigate how Parkin and PGC-1α activity determine the density and morphology of mitochondria in dopaminergic neurons, we performed a transmission electron microscopy (TEM) analysis on neuronal soma in the SN *pars compacta*, four months after vector injection. SN injected with either AAV-Parkin, AAV-PGC-1α, or the two vectors together, were compared to the control, non-injected hemisphere (Fig. 7A).

We measured cytosolic mitochondrial density inside the soma of nigral neurons. Compared to control neuronal cell bodies, PGC-1α induced a significant increase in mitochondrial density (+53%; Fig. 7B). In contrast, overexpression of Parkin alone did not induce any significant change in the number of mitochondria. Nevertheless, compared to neurons overexpressing PGC-1α, co-expression of Parkin and PGC-1α normalized the density of mitochondria in the soma of nigral neurons.

Next, we analysed the effect of PGC-1α and Parkin on mitochondrial morphology. Two parameters were used: the circularity of mitochondrial sections, which has an inverse relationship with the elongation of this organelle (45), and the surface of individual mitochondria sections. The overexpression of PGC-1α led to an increase of the average surface of mitochondrial sections, while Parkin did not appear to have any major effect on this parameter (Fig. 7A and D). However, Parkin significantly reduced the circularity of neuronal mitochondria in the SN co-injected with the PGC-1α vector (Fig. 7C). Collectively, the neurons co-expressing Parkin and PGC-1α displayed more elongated mitochondria, contrasting with the enlarged round mitochondria found following expression of PGC-1α alone (Fig. 7A and D). Furthermore, we noticed that the distribution of the sizes of individual mitochondria in neurons co-expressing Parkin and PGC-1α was more homogenous and remained closer to the control condition (Fig. 7D). Overall, while PGC-1α overexpression increases the density and size of mitochondria in the soma of nigral dopaminergic neurons, the mitochondria are more sparse and elongated when Parkin is co-expressed.

Parkin and PGC-1α regulate the interaction of mitochondria with the endoplasmic reticulum

The interaction between mitochondria and the ER is critical for the dynamics of mitochondria (46). In addition, the tethering of mitochondria to the ER depends on Mfn2 (47), which appears to be a key factor under the control of Parkin and PGC-1α. Next, we assessed in nigral neurons the abundance of contacts formed by the mitochondrial outer membrane with the ER (MAM) (Fig. 8A and B). The mitochondria-ER association was analysed by measuring the proportion of mitochondrial sections making contacts with the ER membrane (Fig. 8B). We found that PGC-1α had a strong effect on the presence of MAMs. In the SN injected with AAV-PGC-1α, the proportion of mitochondria associated

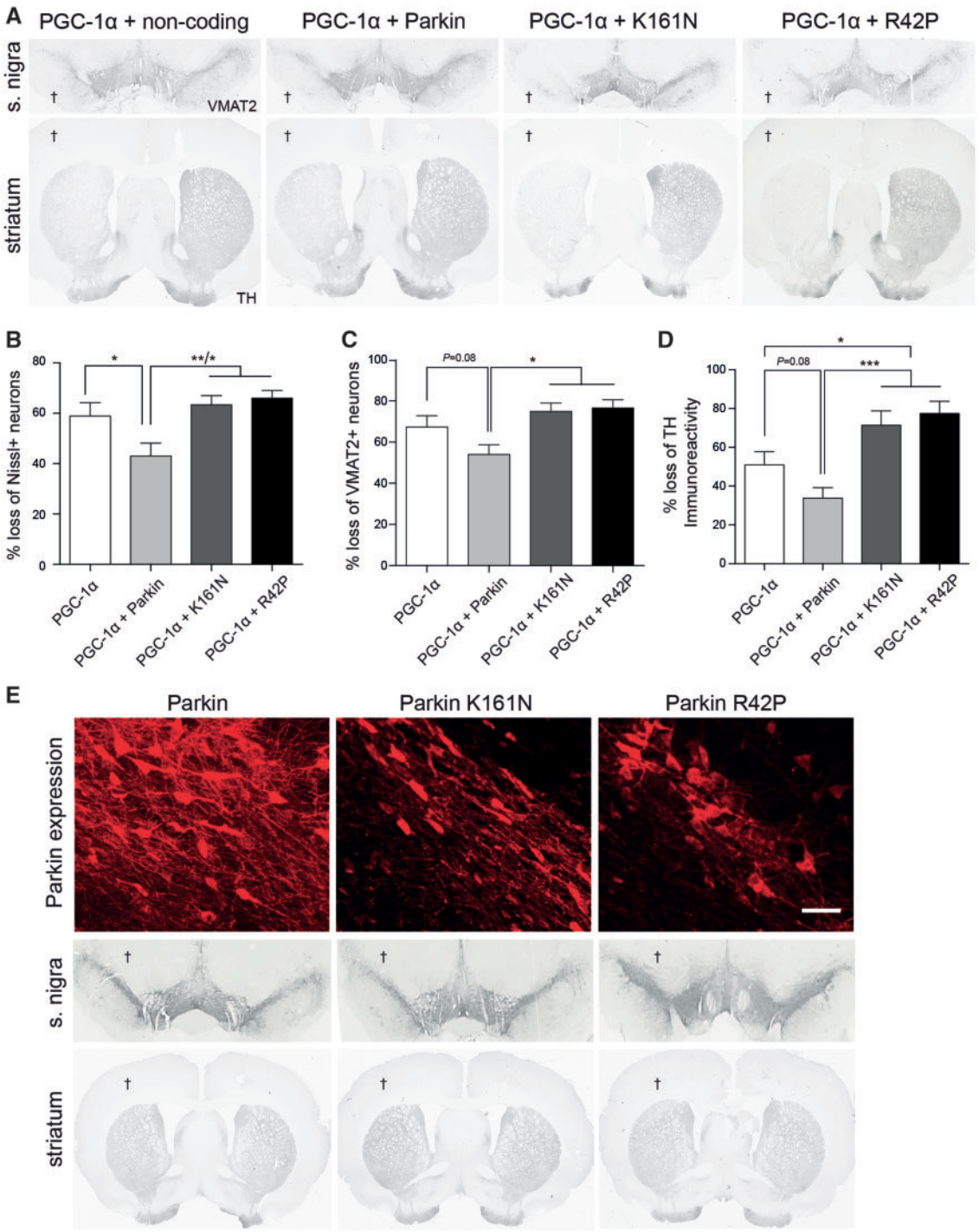

Figure 6. *In vivo*, the expression of PGC-1α reveals differential effects on the survival of nigral dopaminergic neurons between wild-type Parkin and the R42P and K161N mutated forms. An AAV2/6 vector encoding PGC-1α was co-injected in the rat *substantia nigra* with either a non-coding vector, AAV-Parkin, AAV-Parkin K161N or AAV-Parkin R42P. The nigrostriatal system was analysed 4 months post-injection. (**A**) Representative images of tyrosine hydroxylase (TH) immunostainings at the level of the *substantia nigra* (upper panels) and *striatum* (lower panels). Wild-type Parkin and the mutated forms were compared under conditions where PGC-1α was overexpressed in the *substantia nigra*. Dagger sign (†) indicates the side ipsilateral to the injection. (**B**) Quantification of the loss of Nissl-positive neurons (**C**) Quantification of the loss of VMAT2-positive neurons. (**D**) Quantification of the loss of TH immunoreactivity in the *striatum* by densitometry analysis. All data are expressed as the mean ± SEM of the % loss in the hemisphere ipsilateral to the injection versus the contralateral non-injected hemisphere. PGC-1α control: $n = 5$; PGC-1α+Parkin: $n = 8$; PGC-1α+K161N: $n = 7$; PGC-1α+R42P: $n = 6$. $^{*}P < 0.05$, $^{**}P < 0.01$, $^{***}P < 0.001$. One-way ANOVA, Newman-Keuls multiple comparison post-hoc test. (**E**) Representative images of Parkin (upper panels) and TH immunostainings at the level of the *substantia nigra* (middle panels) and *striatum* (lower panels). Overexpression of wild-type Parkin or the mutants were compared in the absence of PGC-1α overexpression. Dagger sign (†) indicates the side ipsilateral to the injection. Scale bar: 50 μM.

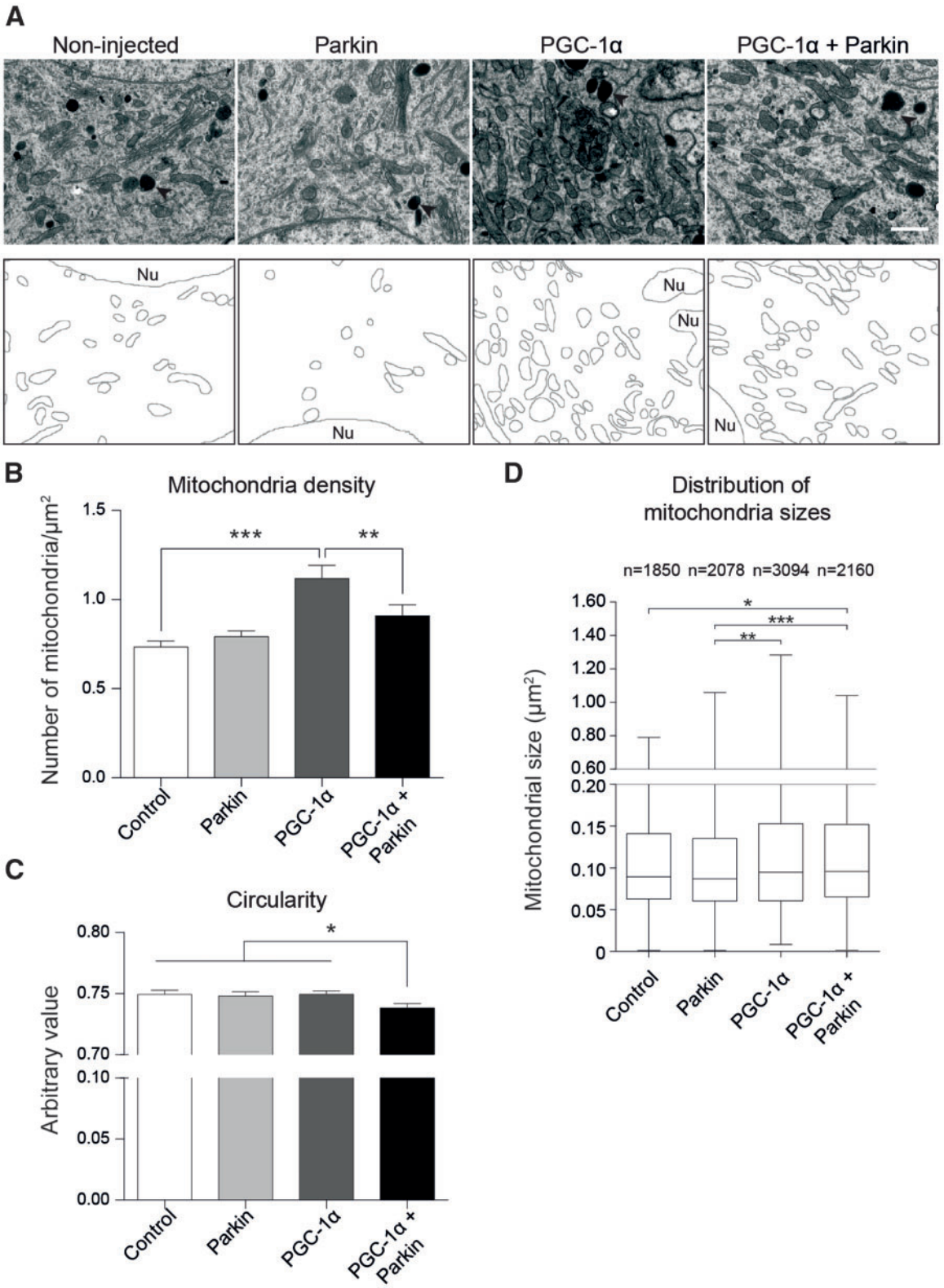

Figure 7. Co-expression of Parkin improves mitochondrial morphology and reduces mitochondrial density in the soma of nigral dopaminergic neurons overexpressing PGC-1α. (**A**) Representative TEM images of the cytosol in the soma of rat dopaminergic neurons. Neurons from the non-injected hemisphere, PGC-1α, Parkin and PGC-1α+Parkin groups are shown for comparison (upper panels). The filled arrowhead indicates a lipofuscin granule. The lower panels show the segmentation of mitochondria. Scale bar: 2 μm. (**B**) Mitochondrial density expressed as the number of mitochondria per μm^2 of cytosol area ($n = 24$ neurons per condition). (**C**) Circularity of mitochondria was measured as an indicator of the elongation of the organelle. (**D**) Box-and-whisker plot showing the distribution of the sizes of individual mitochondria in each group. TEM analysis was performed on three separate animals in each group. For (C-E), the number of individual mitochondria measured in each condition is indicated on graph E. In (B-D), data represent the mean ± SEM. One-way ANOVA, Newman-Keuls multiple comparison post-hoc test for (B) and Fischer's LSD post-hoc test for (C). Kruskal-Wallis test followed by Dunn's multiple comparison test for (D). $^*P < 0.05$, $^{**}P < 0.01$, $^{***}P < 0.001$.

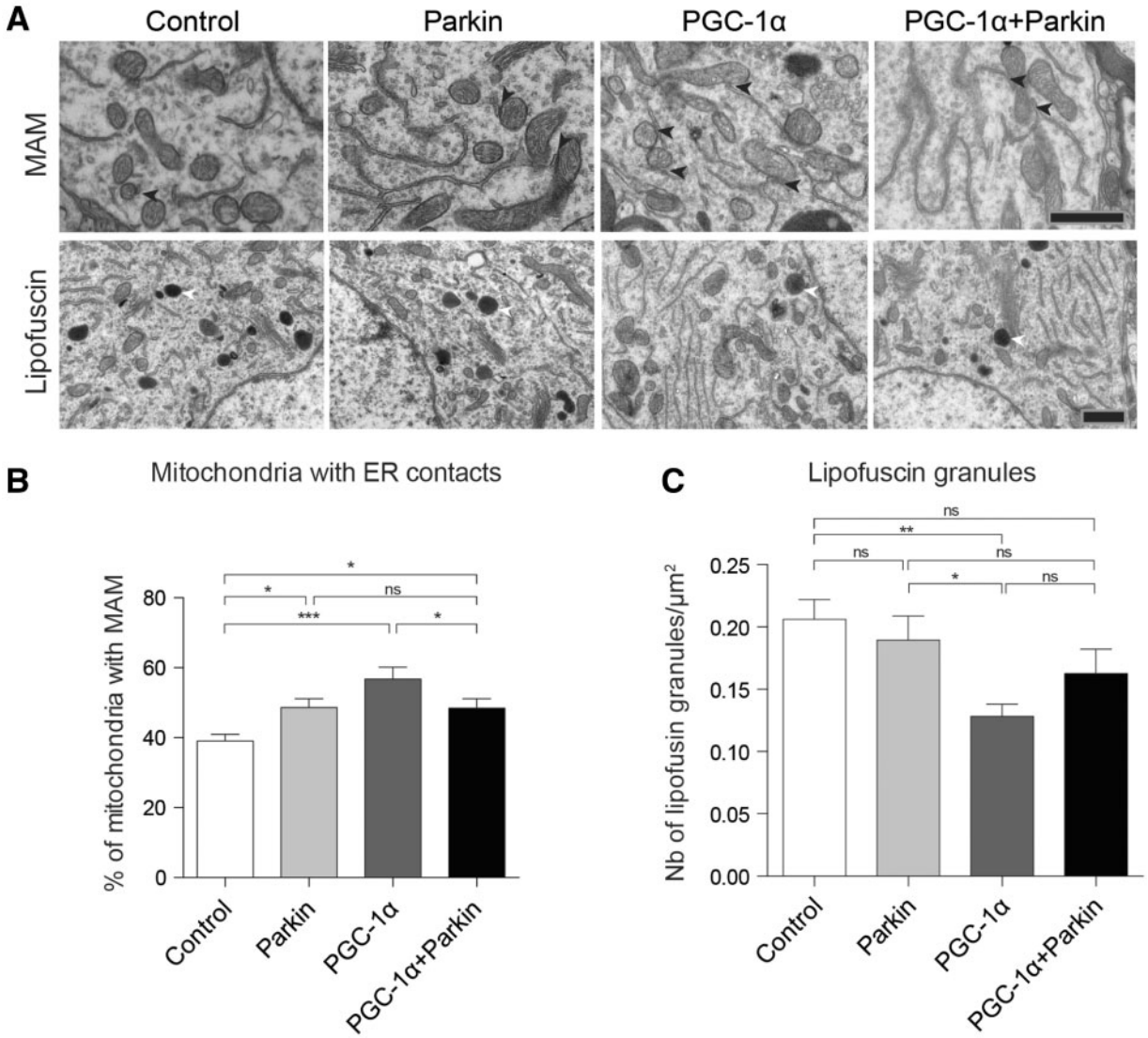

Figure 8. PGC-1α increases the number of mitochondria-ER contacts, which is normalized by the co-expression of Parkin. (**A**) Representative images of mitochondria in contact with the ER membranes (MAMs, filled arrowheads, upper panel). Pictures of typical lipofuscin granules are shown in the lower panel (white arrowheads). Scale bar: 1 μm. (**B**) Percentage of mitochondria in contact with ER membranes ($n = 24$ neurons per condition). (**C**) Density of lipofuscin granules per μm^2 of cytosol area ($n = 24$ neurons per condition). One-way ANOVA and Newman-Keuls multiple comparison post-hoc test for (B) and (C). $^*P < 0.05$, $^{**}P < 0.01$, $^{***}P < 0.001$, ns non-significant.

with the ER was significantly increased to 57 ± 3%, compared to the non-injected contralateral SN (39 ± 2%). Remarkably, co-expression of Parkin counterbalanced the effects seen with PGC-1α alone. In the SN co-injected with the PGC-1α and Parkin vectors, MAM density was similar to when Parkin was overexpressed on its own. Overexpression of Parkin alone only slightly increased the percentage of mitochondria with MAM compared to control. These results suggest that Parkin activity may oppose the effects of PGC-1α on MAMs, possibly via the ubiquitylation of Mfn2.

Next, we sought to explore in nigral dopaminergic neurons possible changes in lipofuscin deposition, an indicator of lysosomal activity, which has been linked to mitochondrial turnover. The number of lipofuscin granules was significantly decreased in nigral neurons overexpressing PGC-1α, which may indicate PGC-1α-induced changes in the autophagic degradation of organelles including mitochondria (Fig. 8C). In neurons overexpressing Parkin, PGC-1α did not lead to any significant difference in the number of lipofuscin granules.

Overall, Parkin appears to improve mitochondrial morphology in dopaminergic neurons overexpressing PGC-1α, mainly by normalizing mitochondrial density, promoting the elongation of mitochondria and reducing the number of contacts with the ER.

Discussion

We explored in neuronal cells the effects of co-expressing Parkin and the transcriptional co-regulator PGC-1α on the mitochondrial function. We found that co-expression of Parkin and PGC-1α induces mitochondrial turnover, exceeding the effects seen with PGC-1α alone. Furthermore, PGC-1α modifies the effects of Parkin on mitochondrial quality control and function. While Parkin alone decreases maximal respiratory rate in neuronal cells, Parkin in combination with PGC-1α enhances the

mitochondrial maximal respiration rate and reserve respiratory capacity. Neurons co-expressing PGC-1α and Parkin showed a faster recovery of their mitochondrial membrane potential after CCCP exposure. Parkin and PGC-1α enhanced the transcription of mitochondrial genes including *Tfam*. Remarkably, PGC-1α also increased the degradation of Mfn2, a key ubiquitylation target of Parkin at the surface of mitochondria. *In vivo*, Parkin was found to mitigate the negative effects induced by the continuous overexpression of PGC-1α in the rat nigrostriatal system. Co-expression of Parkin significantly protects the nigral dopaminergic neurons. This effect is consistent with the presence of more elongated and more sparse mitochondria in the neuronal soma. Parkin also normalizes the mitochondria-ER interactions.

The Parkin/PGC1α axis and mitochondrial turnover

It has been shown that Parkin controls mitochondrial mass by inducing the proteasomal degradation of PARIS, a transcription repressor of PGC-1α (25). Here, we show that co-expression of Parkin and PGC-1α leads to a dramatic increase in mitochondrial numbers in neuronal cells. As the effect of Parkin on mitochondrial density is abolished in PGC-1α null neurons (Fig. 1C), PGC-1α is likely to play a primary role in Parkin-induced mitochondria biogenesis. However, the additive effect of Parkin is not only explained by increased PGC-1α transcription via PARIS degradation. Indeed, Parkin can promote the expression of genes implicated in mitochondria biogenesis and OXPHOS. Parkin directly interacts with Tfam, a mitochondrial transcription factor that induces mtDNA replication and transcription of mitochondrial genes (48). More recently, Parkin and PINK1 have also been shown to control the translation of components of the respiratory chain on the outer mitochondrial membrane (49). Here, Parkin further enhances the transcription of *Tfam* and *Ndufs1* in neurons expressing PGC-1α. Remarkably, PGC-1α overexpression also promotes the effect of Parkin on mitophagy in SH-SY5Y neuroblastoma cells. These factors that promote mitochondrial biogenesis and mitophagy appear to have coordinated functions in neurons. Parkin and PGC-1α are therefore critical factors, which control mitochondrial turnover and quality in conditions of mitochondrial stress.

Parkin and mitochondrial respiration

The role of Parkin in mitochondrial respiration has been previously shown in different models. Mice deficient for either Parkin or PINK1 display signs of mitochondrial dysfunction (50,51), and the maximal mitochondrial respiration is decreased in the *striatum* of Parkin null mice (51,52). More recently, defects in mitochondrial respiration have been reported in neurons following Parkin knockdown, or overexpression of the PGC-1α repressor PARIS, which is linked to Parkin deficiency (25). In *Drosophila*, the loss of either Parkin or PINK1 reduces the turnover of many mitochondrial respiratory chain subunits (53). Here, we find that the effect of Parkin on mitochondrial respiration depends on PGC-1α expression. Only when Parkin is co-expressed with PGC-1α do the neurons show a significant increase in the CCCP-induced maximal respiration. Therefore, Parkin likely cooperates with PGC-1α in controlling OXPHOS.

Parkin and mitochondrial repair

Repair mechanisms may be important to the homeostasis of mitochondria in neurons, particularly when these organelles are located distally to the cell body. In neurons co-expressing Parkin and PGC-1α, we observed a protection of $\Delta\psi m$ in mitochondria transiently exposed to an uncoupling agent (Fig. 3A). This effect is consistent with the observed increase in maximal respiration, which may facilitate the recovery of the membrane potential. PGC-1α could contribute to this effect by promoting the synthesis of proteins involved in OXPHOS, in conjunction with Parkin. Furthermore, Parkin may control the turnover of the respiratory complexes located in the inner mitochondrial membrane, although the mechanisms remain unclear. The ubiquitin-proteasome system controls the quality of mitochondrial components 1) by targeting proteins before or during their import into the organelle, or 2) via the retrotranslocation and degradation of mitochondrial proteins (54). Parkin-dependent ubiquitination is found on proteins located inside the organelle following mitochondria depolarization (37). Furthermore, Parkin induces the biogenesis of MDVs following oxidative stress within mitochondria (55). MDVs contain damaged mitochondrial proteins, and may contribute to their lysosomal degradation, highlighting another role of Parkin in the control of mitochondrial quality.

Parkin may also cooperate with PGC-1α in maintaining mitochondrial genome integrity (48,56,57). We indeed measured higher mtDNA copy numbers in neurons overexpressing both PGC-1α and Parkin following 24 h of CCCP exposure (Fig. 3B). Overall, the concerted action of Parkin and PGC-1α promotes the synthesis and quality control of mitochondrial proteins, mtDNA replication and repair, as well as the incorporation of lipids inside the mitochondria (58), which collectively ensure the proper function of this organelle.

PGC-1α and Parkin regulate the level of Mfn2

Parkin targets preferentially targets proteins associated with the mitochondrial outer membrane, such as VDAC1 and mitofusins (37). Upon mitochondrial depolarization, Parkin ubiquitylates mitofusins and promotes their degradation in a proteasome- and p97 (AAA+ ATPase)-dependent manner (59). In SH-SY5Y neuroblastoma cells, PGC-1α induces Mfn2 degradation independently of Parkin, and in the absence of any mitochondrial stressor (Fig. 5). This effect is likely to be mediated by the induced expression of factors controlling the turnover of Mfn2. MUL1 can compensate for the loss of PINK1/Parkin function via the ubiquitin-dependent degradation of Mitofusin. Therefore, it might act in parallel to the PINK1/Parkin pathway on the mitochondrial quality control (60). Although PGC-1α up-regulates the expression of MUL1, it is needed to further explore the factors implicated in the induced degradation of Mfn2. As PGC-1α also up-regulates Mfn2 transcription (Fig. 4), it may increase the overall turnover of this protein, which could have important effects on the dynamics of mitochondria (61), their interaction with the ER (62) and their transport along the axon (63). Remarkably, a recent study has shown that the Mfn2 level is specifically increased at the MAM fraction isolated from the liver of Parkin null mice (64).

The suppression of Mfn2 in the nigrostriatal dopaminergic system of floxed mice leads to a neurodegenerative phenotype characterized by severe loss of dopamine marker expression and decreased dopamine content in the *striatum* (65). This phenotype resembles what is observed in the nigrostriatal system of rats and mice continuously overexpressing PGC-1α (43,66). Moreover, dopaminergic neurons deficient for Mfn2 accumulate enlarged, spherical mitochondria (65), which are similar to the

ones observed in rats overexpressing PGC-1α (Fig. 7). Therefore, it is plausible that the increased degradation of Mfn2 induced by PGC-1α contributes to the defects observed *in vivo*.

In vivo effects of Parkin in nigral neurons expressing PGC-1α

Parkin and PINK1 null mice have failed to recapitulate the degeneration of dopaminergic neurons in the SN (67–69). Furthermore, the loss of Parkin does not worsen the neurodegenerative phenotype of MitoPark mice (70). Nevertheless, Parkin activity is critical to the survival of nigral dopaminergic neurons in Mutator mice, which have an accelerated mutation rate in mtDNA (71). It is intriguing that Parkin enhances the survival and function of nigral dopaminergic neurons chronically overexpressing PGC-1α. Ultrastructural analysis has revealed a dramatic increase in mitochondria density in the soma of nigral dopaminergic neurons overexpressing PGC-1α (Fig. 7B). This excess of mitochondria may create a situation where mitochondrial quality control is critically needed. Parkin reduces mitochondria density in nigral neurons expressing PGC-1α, in contrast to the increased number of mitochondria observed in mouse cortical neurons (Fig. 1). Continuous PGC-1α expression in nigral dopaminergic neurons generates conditions that may challenge the quality control of mitochondria. In SH-SY5Y cells exposed to CCCP, the co-expression of Parkin and PGC-1α leads to robust mitophagic activity. Mitochondrial turnover could be similarly enhanced in nigral neurons co-expressing these two factors. In these neurons, mitochondria may indeed be exposed to chronic oxidative stress caused by dopamine metabolism, prompting the degradation of defective organelles. Furthermore, dopaminergic neurons have a unique morphology, with long axons and an extremely large number of synaptic connections (2). Hence, the distribution of mitochondria inside the neurites is critically important. The density of mitochondria in the neuronal soma does not necessarily reflect the overall number of mitochondria present in nigral dopaminergic neurons.

Overall, we find that Parkin preserves mitochondrial homeostasis and enhances mitochondrial activity via its functional interaction with PGC-1α. Overall, the Parkin-PGC-1α axis has effects beyond the upregulation of PGC-1α transcription. In particular, the combined action of Parkin and PGC-1α appears as a potent regulator of mitochondrial biogenesis and quality control. This could have important implications in PD, as nigral dopaminergic neurons may critically depend on mitochondrial activity for their function and survival.

Materials and Methods

Primers, plasmids and antibodies

For the source of the antibodies and primer sequences, see the Supplemental Information (Supplementary Materials, Table S1 and S2). The plasmids are also described in the Supplemental Information.

Animals

For the source of animals, see the Supporting Information. All animals were housed in a 12 h light/dark cycle, with *ad libitum* access to food and water. All procedures were performed in accordance with Swiss legislation and the European Community Council directive (86/609/EEC) for the care and use of laboratory animals.

Production and titration of adeno-associated viral vectors

QuikChange Multi Site-Directed Mutagenesis Kit (Agilent Technologies) was used to generate the K161N and R42P Parkin mutants. The plasmid pRK5-HA-Parkin encoding HA-tagged human Parkin was used as a template. The Parkin cDNAs carrying the mutations were amplified by PCR and subcloned into the AAV-PGK-MCS plasmid using standard procedures. Methods for the production and the titration of AAV2/6 vectors have been previously described in details (72). The infectivity titer of each vector was determined by real-time (rt) PCR (see Supplemental Information).

Western blot analysis

SH-SY5Y cells were lysed with NP-40 lysis buffer (1% NP-40, 150 mM NaCl, 50 mM Tris-Cl, pH 8.0) supplemented with cocktails of protease (Roche) and phosphatase inhibitors (Sigma). Protein samples were analysed by SDS-PAGE using standard procedures (see Supplemental Information).

Primary cortical neuron culture

Cortical neurons were dissected from E16 C57BL/6J mouse embryos (Janvier). Similar procedures were applied to obtain primary cortical neurons from genetically modified mice (see Supplemental Information).

Analysis of mRNA expression

Total mRNA was extracted using the Maxwell® 16 LEV simplyRNA Cells Kit (Promega), according to the manufacturer's instructions. For reverse-transcription and PCR reaction, see Supplemental Information.

Mitochondria DNA quantification

Total DNA was extracted from neurons cultured in 24-well plates using the Maxwell® 16 Viral Total Nucleic Acid Purification Kit (Promega), according to the manufacturer's instructions. For each sample, 10 ng of total DNA was applied as a template in the rt-PCR reaction. Primers used are summarized in Supplementary Material, Table S2. The Rotor-Gene SYBR Green PCR kit (Qiagen) master mix was applied for rt-PCR DNA amplifications, which were analysed using an Applied Biosystems 7900HT Fast Real-Time PCR System. The ratio between mtDNA (*Mt-co2*, *16S*) and genome DNA (*Ucp2*, *Hk2*) was calculated using the ΔΔCT method.

Mitophagy index

The plasmid encoding the mitochondria-targeted m-Keima (pCHAC-mt-mKeima) was purchased from Addgene (#72342). To quantify mitophagy in individual cells, the m-Keima signal was imaged by live confocal microscopy. For imaging, cells were plated on glass coverslips and incubated in DMEM without phenol red, supplemented with 10% FBS and penicillin/streptomycin. Fluorescent samples were examined with a Zeiss LSM 710 confocal microscope (Carl Zeiss MicroImaging) equipped with a

Plan-Apochromat 20×/0.8 NA and 40×/1.3 NA oil immersion objective lens. m-Keima fluorescence was imaged in two channels via two sequential excitations (458 nm, cyan; 561 nm, red) and using a 580- to 700-nm emission range. Laser power was set at the lowest intensity that would allow clear visualization of the m-Keima signal. Imaging settings were kept identical for all experimental conditions. Mitophagy quantification was performed as previously described (73). Briefly, regions were defined manually for fluorescence and area measurements, on groups of whole cells. For each region measured, the mitophagy index was calculated as the ratio of the integrated density signals [561 nm/(561 nm + 458 nm)], each value corrected for background using a control condition not transfected with the m-Keima plasmid. The average of 7 to 9 independent regions, representing 20–30 cells in total, was measured for each condition. An arbitrary value of one was assigned to the average of the control condition +CCCP, and all samples were normalized to this value.

Flow cytometry analysis

Neurons infected with AAV2/6-MitoDsRed were resuspended in 100 µL Neurobasal medium without phenol red (Life Technologies). Neurons were dissociated with a gentle pipette trituration. The cells were analysed using an Accuri C6 flow cytometer (BD biosciences). Forward and side light scatters were used to gate the population of living cells. The fluorescent signal was acquired in FL2 channel, followed by analysis in software CFlow®SAMPLER. FL2 gating was consistently applied across samples to exclude MitoDsRed-negative cells. Final data were represented as mean red fluorescence for single events in each sample.

Oxygen consumption measurement

Neurons were seeded in XF96 Polystyrene Cell Culture Microplates (Seahorse Bioscience) and infected with viral vectors. Two days before measurement, 75% of the culture medium was replaced by Neurobasal A medium (Gibco), supplemented with 2 mM glucose, 25 mM pyruvate, 100 U/mL Penicillin-Streptomycin, 2 mM Glutamax and B27. For the details of measurement, see Supplemental Information.

Mitochondria membrane potential measurement

The MitoProbe™ JC-1 Assay Kit (Life Technologies) was used to assess the mitochondrial membrane potential ($\Delta\psi m$). All procedures followed the manufacturer's instructions. See Supplemental Information for details.

Stereotaxic injection

Stereotaxic injections of the AAV2/6 vectors in the rat SN were performed as previously described (43). See Supplemental Information for details.

Behavioural test

Ipsiversive rotations induced by intraperitoneal injection of amphetamine (D-amphetamine sulfate, 2.5 mg/kg; Sigma) were measured in individual rats to assess asymmetry in the dopamine signalling in the basal ganglia. The procedure was carried out as described previously (43). Rotametry was performed before vector injection (pre-test), and was repeated at 2 and 4 months post-injection.

Histology and quantification

Animals were sacrificed four months post-vector injection and brain tissue was processed as described previously (72). See Supplemental Information for details.

Transmission electron microscopy

Four months post-injection, animals were deeply anaesthetized, perfused, and subjected to electron microscopy analysis. See Supplemental Information for details.

Three animals were used for each condition. For relative quantification of changes in organelle morphology, 50 nm-thick sections from the SN *pars compacta* were systematically imaged in a transmission electron microscope (FEI Company) operated at 80 kV. For each SN, we analysed eight randomly chosen large-size neuronal soma, identified by the presence of the cell nucleus. Dopaminergic neurons were recognized based on their morphology. Cellular and nuclear membranes, as well as mitochondria were outlined manually using the ImageJ software. Mitochondria number, size and circularity were measured using the Particle Analyzer tool. Mitochondria density is represented as the number of mitochondria normalized to the measured surface of the cytosol. The size and circularity of mitochondria were measured for each individual organelle, which was considered as a replicate for statistical analysis. Lipofuscin granules and MAMs were labelled and quantified using Cell Counter tool. MAM was defined as a close contact between mitochondria and ER (< 20 nm).

Statistics

Data are presented as average ± standard error of the mean (SEM). Statistical analysis was performed using the prism 6 software (version 6.0c). Two-tailed unpaired homoscedastic Student's *t*-test, one- and two-way ANOVA followed by Fischer's LSD or Newman-Keuls multiple comparison post-hoc test were applied for analysing data with normal distribution. Kruskal-Wallis test followed by Dunn's multiple comparison post-hoc test was applied for mitochondria size. The alpha level of significance was set at 0.05. In most figures, only the statistically different comparisons are indicated. Number of replicates for each experiment, as well as statistical tests, are indicated in the Figure legends.

Supplementary Material

Supplementary Material is available at *HMG* online.

Acknowledgements

The authors thank Dr. Herman van der Putten for editing the manuscript, Philippe Colin and Christel Sadeghi for their expert technical support in animal experimentation and histology, as well as Aline Aebi, Fabienne Pidoux and Vivianne Padrun for viral vector production.

Conflict of Interest Statement: None declared.

Funding

This work was supported by Swiss National Science Foundation [grant numbers 31003A_120653, 31003A_135696]. NBM was supported by the Neuromuscular Research Association Basel (NeRAB). DD was supported by a fellowship funded by Associazione Italiana per la Ricerca sul Cancro (AIRC) and Marie Curie Actions. JA, NM and DD were supported by the Swiss National Science Foundation [grant number 31003A-140780] and by Systems X [grant number SySX.ch 2013/153]. All authors received funding from EPFL.

References

1. Miyazaki, I. and Asanuma, M. (2008) Dopaminergic neuron-specific oxidative stress caused by dopamine itself. *Acta Med. Okayama*, **62**, 141–150.
2. Bolam, J.P. and Pissadaki, E.K. (2012) Living on the edge with too many mouths to feed: why dopamine neurons die. *Mov. Disord.*, **27**, 1478–1483.
3. Winklhofer, K.F. and Haass, C. (2010) Mitochondrial dysfunction in Parkinson's disease. *Biochim. Biophys. Acta*, **1802**, 29–44.
4. Porras, G., Li, Q. and Bezard, E. (2012) Modeling Parkinson's disease in primates: The MPTP model. *Cold Spring Harb. Perspect. Med.*, **2**, a009308.
5. Abbas, N., Lucking, C.B., Ricard, S., Durr, A., Bonifati, V., De Michele, G., Bouley, S., Vaughan, J.R., Gasser, T., Marconi, R., *et al.* (1999) A wide variety of mutations in the parkin gene are responsible for autosomal recessive parkinsonism in Europe. French Parkinson's Disease Genetics Study Group and the European Consortium on Genetic Susceptibility in Parkinson's Disease. *Hum. Mol. Genet.*, **8**, 567–574.
6. Periquet, M., Latouche, M., Lohmann, E., Rawal, N., De Michele, G., Ricard, S., Teive, H., Fraix, V., Vidailhet, M., Nicholl, D., *et al.* (2003) Parkin mutations are frequent in patients with isolated early-onset parkinsonism. *Brain*, **126**, 1271–1278.
7. Dawson, T.M. and Dawson, V.L. (2010) The role of parkin in familial and sporadic Parkinson's disease. *Mov. Disord.*, **25 Suppl 1**, S32–S39.
8. Jin, S.M. and Youle, R.J. (2012) PINK1- and Parkin-mediated mitophagy at a glance. *J. Cell Sci.*, **125**, 795–799.
9. Narendra, D., Tanaka, A., Suen, D.F. and Youle, R.J. (2008) Parkin is recruited selectively to impaired mitochondria and promotes their autophagy. *J. Cell Biol.*, **183**, 795–803.
10. Kane, L.A., Lazarou, M., Fogel, A.I., Li, Y., Yamano, K., Sarraf, S.A., Banerjee, S. and Youle, R.J. (2014) PINK1 phosphorylates ubiquitin to activate Parkin E3 ubiquitin ligase activity. *J. Cell Biol.*, **205**, 143–153.
11. Riley, B.E. and Olzmann, J.A. (2015) A polyubiquitin chain reaction: parkin recruitment to damaged mitochondria. *PLoS Genet.*, **11**, e1004952.
12. Shiba-Fukushima, K., Arano, T., Matsumoto, G., Inoshita, T., Yoshida, S., Ishihama, Y., Ryu, K.Y., Nukina, N., Hattori, N. and Imai, Y. (2014) Phosphorylation of mitochondrial polyubiquitin by PINK1 promotes Parkin mitochondrial tethering. *PLoS Genet.*, **10**, e1004861.
13. Chen, Y. and Dorn, G.W. 2nd (2013) PINK1-phosphorylated mitofusin 2 is a Parkin receptor for culling damaged mitochondria. *Science*, **340**, 471–475.
14. Gegg, M.E., Cooper, J.M., Chau, K.Y., Rojo, M., Schapira, A.H. and Taanman, J.W. (2010) Mitofusin 1 and mitofusin 2 are ubiquitinated in a PINK1/parkin-dependent manner upon induction of mitophagy. *Hum. Mol. Genet.*, **19**, 4861–4870.
15. Cai, Q., Zakaria, H.M., Simone, A. and Sheng, Z.H. (2012) Spatial parkin translocation and degradation of damaged mitochondria via mitophagy in live cortical neurons. *Curr. Biol.*, **22**, 545–552.
16. Van Laar, V.S., Arnold, B., Cassady, S.J., Chu, C.T., Burton, E.A. and Berman, S.B. (2011) Bioenergetics of neurons inhibit the translocation response of Parkin following rapid mitochondrial depolarization. *Hum. Mol. Genet.*, **20**, 927–940.
17. Kornmann, B. (2014) Quality control in mitochondria: use it, break it, fix it, trash it. *F1000Prime Rep.*, **6**, 15.
18. Andreux, P.A., Houtkooper, R.H. and Auwerx, J. (2013) Pharmacological approaches to restore mitochondrial function. *Nat. Rev. Drug Discov.*, **12**, 465–483.
19. Yu, W., Sun, Y., Guo, S. and Lu, B. (2011) The PINK1/Parkin pathway regulates mitochondrial dynamics and function in mammalian hippocampal and dopaminergic neurons. *Hum. Mol. Genet.*, **20**, 3227–3240.
20. Birsa, N., Norkett, R., Wauer, T., Mevissen, T.E., Wu, H.C., Foltynie, T., Bhatia, K., Hirst, W.D., Komander, D., Plun-Favreau, H., *et al.* (2014) Lysine 27 ubiquitination of the mitochondrial transport protein Miro is dependent on serine 65 of the Parkin ubiquitin ligase. *J. Biol. Chem.*, **289**, 14569–14582.
21. Mortiboys, H., Thomas, K.J., Koopman, W.J., Klaffke, S., Abou-Sleiman, P., Olpin, S., Wood, N.W., Willems, P.H., Smeitink, J.A., Cookson, M.R., *et al.* (2008) Mitochondrial function and morphology are impaired in parkin-mutant fibroblasts. *Ann. Neurol.*, **64**, 555–565.
22. Moore, D.J. (2006) Parkin: a multifaceted ubiquitin ligase. *Biochem. Soc. Trans.*, **34**, 749–753.
23. Shin, J.H., Ko, H.S., Kang, H., Lee, Y., Lee, Y.I., Pletinkova, O., Troconso, J.C., Dawson, V.L. and Dawson, T.M. (2011) PARIS (ZNF746) repression of PGC-1alpha contributes to neurodegeneration in Parkinson's disease. *Cell*, **144**, 689–702.
24. Palikaras, K. and Tavernarakis, N. (2014) Mitochondrial homeostasis: the interplay between mitophagy and mitochondrial biogenesis. *Exp. Gerontol.*, **56**, 182–188.
25. Stevens, D.A., Lee, Y., Kang, H.C., Lee, B.D., Lee, Y.I., Bower, A., Jiang, H., Kang, S.U., Andrabi, S.A., Dawson, V.L., *et al.* (2015) Parkin loss leads to PARIS-dependent declines in mitochondrial mass and respiration. *Proc. Natl. Acad. Sci. U S A*, **112**, 11696–11701.
26. Poole, A.C., Thomas, R.E., Andrews, L.A., McBride, H.M., Whitworth, A.J. and Pallanck, L.J. (2008) The PINK1/Parkin pathway regulates mitochondrial morphology. *Proc. Natl. Acad. Sci. U S A*, **105**, 1638–1643.
27. Deng, H., Dodson, M.W., Huang, H. and Guo, M. (2008) The Parkinson's disease genes pink1 and parkin promote mitochondrial fission and/or inhibit fusion in Drosophila. *Proc. Natl. Acad. Sci. U S A*, **105**, 14503–14508.
28. Soriano, F.X., Liesa, M., Bach, D., Chan, D.C., Palacin, M. and Zorzano, A. (2006) Evidence for a mitochondrial regulatory pathway defined by peroxisome proliferator-activated receptor-gamma coactivator-1 alpha, estrogen-related receptor-alpha, and mitofusin 2. *Diabetes*, **55**, 1783–1791.
29. Zheng, B., Liao, Z., Locascio, J.J., Lesniak, K.A., Roderick, S.S., Watt, M.L., Eklund, A.C., Zhang-James, Y., Kim, P.D., Hauser, M.A., *et al.* (2010) PGC-1alpha, a potential therapeutic target for early intervention in Parkinson's disease. *Sci. Transl. Med.*, **2**, 52ra73.

30. Corona, J.C. and Duchen, M.R. (2015) PPARgamma and PGC-1alpha as therapeutic targets in Parkinson's. *Neurochem. Res.*, **40**, 308–316.
31. Soyal, S.M., Felder, T.K., Auer, S., Hahne, P., Oberkofler, H., Witting, A., Paulmichl, M., Landwehrmeyer, G.B., Weydt, P., Patsch, W., *et al.* (2012) A greatly extended PPARGC1A genomic locus encodes several new brain-specific isoforms and influences Huntington disease age of onset. *Hum. Mol. Genet.*, **21**, 3461–3473.
32. Katayama, H., Kogure, T., Mizushima, N., Yoshimori, T. and Miyawaki, A. (2011) A sensitive and quantitative technique for detecting autophagic events based on lysosomal delivery. *Chem. Biol.*, **18**, 1042–1052.
33. Shokolenko, I., Venediktova, N., Bochkareva, A., Wilson, G.L. and Alexeyev, M.F. (2009) Oxidative stress induces degradation of mitochondrial DNA. *Nucleic Acids Res.*, **37**, 2539–2548.
34. Suzuki-Karasaki, M., Ochiai, T. and Suzuki-Karasaki, Y. (2014) Crosstalk between mitochondrial ROS and depolarization in the potentiation of TRAIL-induced apoptosis in human tumor cells. *Int. J. Oncol.*, **44**, 616–628.
35. Choi, C.S., Befroy, D.E., Codella, R., Kim, S., Reznick, R.M., Hwang, Y.J., Liu, Z.X., Lee, H.Y., Distefano, A., Samuel, V.T., *et al.* (2008) Paradoxical effects of increased expression of PGC-1alpha on muscle mitochondrial function and insulin-stimulated muscle glucose metabolism. *Proc. Natl. Acad. Sci. U S A*, **105**, 19926–19931.
36. Cartoni, R., Leger, B., Hock, M.B., Praz, M., Crettenand, A., Pich, S., Ziltener, J.L., Luthi, F., Deriaz, O., Zorzano, A., *et al.* (2005) Mitofusins 1/2 and ERRalpha expression are increased in human skeletal muscle after physical exercise. *J. Physiol.*, **567**, 349–358.
37. Sarraf, S.A., Raman, M., Guarani-Pereira, V., Sowa, M.E., Huttlin, E.L., Gygi, S.P. and Harper, J.W. (2013) Landscape of the PARKIN-dependent ubiquitylome in response to mitochondrial depolarization. *Nature*, **496**, 372–376.
38. Colombini, M. (2004) VDAC: the channel at the interface between mitochondria and the cytosol. *Mol. Cell. Biochem.*, **256-257**, 107–115.
39. Papanicolaou, K.N., Khairallah, R.J., Ngoh, G.A., Chikando, A., Luptak, I., O'Shea, K.M., Riley, D.D., Lugus, J.J., Colucci, W.S., Lederer, W.J., *et al.* (2011) Mitofusin-2 maintains mitochondrial structure and contributes to stress-induced permeability transition in cardiac myocytes. *Mol. Cell. Biol.*, **31**, 1309–1328.
40. Wang, W., Zhang, F., Li, L., Tang, F., Siedlak, S.L., Fujioka, H., Liu, Y., Su, B., Pi, Y. and Wang, X. (2015) MFN2 couples glutamate excitotoxicity and mitochondrial dysfunction in motor neurons. *J. Biol. Chem.*, **290**, 168–182.
41. Berman, S.B. and Hastings, T.G. (1999) Dopamine oxidation alters mitochondrial respiration and induces permeability transition in brain mitochondria: implications for Parkinson's disease. *J. Neurochem.*, **73**, 1127–1137.
42. Pissadaki, E.K. and Bolam, J.P. (2013) The energy cost of action potential propagation in dopamine neurons: clues to susceptibility in Parkinson's disease. *Front. Comput. Neurosci.*, **7**, 13.
43. Ciron, C., Lengacher, S., Dusonchet, J., Aebischer, P. and Schneider, B.L. (2012) Sustained expression of PGC-1alpha in the rat nigrostriatal system selectively impairs dopaminergic function. *Hum. Mol. Genet.*, **21**, 1861–1876.
44. Jiang, H., Ren, Y., Zhao, J. and Feng, J. (2004) Parkin protects human dopaminergic neuroblastoma cells against dopamine-induced apoptosis. *Hum. Mol. Genet.*, **13**, 1745–1754.
45. Dagda, R.K., Cherra, S.J., 3rd, Kulich, S.M., Tandon, A., Park, D. and Chu, C.T. (2009) Loss of PINK1 function promotes mitophagy through effects on oxidative stress and mitochondrial fission. *J. Biol. Chem.*, **284**, 13843–13855.
46. Rowland, A.A. and Voeltz, G.K. (2012) Endoplasmic reticulum-mitochondria contacts: function of the junction. *Nat. Rev. Mol. Cell. Biol.*, **13**, 607–625.
47. de Brito, O.M. and Scorrano, L. (2008) Mitofusin 2 tethers endoplasmic reticulum to mitochondria. *Nature*, **456**, 605–610.
48. Kuroda, Y., Mitsui, T., Kunishige, M., Shono, M., Akaike, M., Azuma, H. and Matsumoto, T. (2006) Parkin enhances mitochondrial biogenesis in proliferating cells. *Hum. Mol. Genet.*, **15**, 883–895.
49. Gehrke, S., Wu, Z., Klinkenberg, M., Sun, Y., Auburger, G., Guo, S. and Lu, B. (2015) PINK1 and Parkin control localized translation of respiratory chain component mRNAs on mitochondria outer membrane. *Cell Metab.*, **21**, 95–108.
50. Gispert, S., Ricciardi, F., Kurz, A., Azizov, M., Hoepken, H.H., Becker, D., Voos, W., Leuner, K., Muller, W.E., Kudin, A.P., *et al.* (2009) Parkinson phenotype in aged PINK1-deficient mice is accompanied by progressive mitochondrial dysfunction in absence of neurodegeneration. *PLoS One*, **4**, e5777.
51. Palacino, J.J., Sagi, D., Goldberg, M.S., Krauss, S., Motz, C., Wacker, M., Klose, J. and Shen, J. (2004) Mitochondrial dysfunction and oxidative damage in parkin-deficient mice. *J. Biol. Chem.*, **279**, 18614–18622.
52. Damiano, M., Gautier, C.A., Bulteau, A.L., Ferrando-Miguel, R., Gouarne, C., Paoli, M.G., Pruss, R., Auchere, F., L'Hermitte-Stead, C., Bouillaud, F., *et al.* (2014) Tissue- and cell-specific mitochondrial defect in Parkin-deficient mice. *PLoS One*, **9**, e99898.
53. Vincow, E.S., Merrihew, G., Thomas, R.E., Shulman, N.J., Beyer, R.P., MacCoss, M.J. and Pallanck, L.J. (2013) The PINK1-Parkin pathway promotes both mitophagy and selective respiratory chain turnover in vivo. *Proc. Natl. Acad. Sci. U S A*, **110**, 6400–6405.
54. Bohovych, I., Chan, S.S. and Khalimonchuk, O. (2015) Mitochondrial protein quality control: the mechanisms guarding mitochondrial health. *Antioxid. Redox Signal*, **22**, 977–994.
55. McLelland, G.L., Soubannier, V., Chen, C.X., McBride, H.M. and Fon, E.A. (2014) Parkin and PINK1 function in a vesicular trafficking pathway regulating mitochondrial quality control. *Embo J.*, **33**, 282–295.
56. Rothfuss, O., Fischer, H., Hasegawa, T., Maisel, M., Leitner, P., Miesel, F., Sharma, M., Bornemann, A., Berg, D., Gasser, T., *et al.* (2009) Parkin protects mitochondrial genome integrity and supports mitochondrial DNA repair. *Hum. Mol. Genet.*, **18**, 3832–3850.
57. Kao, S.Y. (2009) Regulation of DNA repair by parkin. *Biochem. Biophys. Res. Commun.*, **382**, 321–325.
58. Kim, K.Y. and Sack, M.N. (2012) Parkin in the regulation of fat uptake and mitochondrial biology: emerging links in the pathophysiology of Parkinson's disease. *Curr. Opin. Lipidol.*, **23**, 201–205.
59. Tanaka, A., Cleland, M.M., Xu, S., Narendra, D.P., Suen, D.F., Karbowski, M. and Youle, R.J. (2010) Proteasome and p97 mediate mitophagy and degradation of mitofusins induced by Parkin. *J. Cell Biol.*, **191**, 1367–1380.
60. Yun, J., Puri, R., Yang, H., Lizzio, M.A., Wu, C., Sheng, Z.H. and Guo, M. (2014) MUL1 acts in parallel to the PINK1/parkin pathway in regulating mitofusin and compensates for loss of PINK1/parkin. *Elife*, **3**, e01958.

61. Bach, D., Pich, S., Soriano, F.X., Vega, N., Baumgartner, B., Oriola, J., Daugaard, J.R., Lloberas, J., Camps, M., Zierath, J.R., *et al*. (2003) Mitofusin-2 determines mitochondrial network architecture and mitochondrial metabolism. A novel regulatory mechanism altered in obesity. *J. Biol. Chem.*, **278**, 17190–17197.
62. Filadi, R., Greotti, E., Turacchio, G., Luini, A., Pozzan, T. and Pizzo, P. (2015) Mitofusin 2 ablation increases endoplasmic reticulum-mitochondria coupling. *Proc. Natl. Acad. Sci. U S A*, **112**, E2174–E2181.
63. Misko, A., Jiang, S., Wegorzewska, I., Milbrandt, J. and Baloh, R.H. (2010) Mitofusin 2 is necessary for transport of axonal mitochondria and interacts with the Miro/Milton complex. *J. Neurosci.*, **30**, 4232–4240.
64. Gautier, C.A., Erpapazoglou, Z., Mouton-Liger, F., Muriel, M.P., Cormier, F., Bigou, S., Duffaure, S., Girard, M., Foret, B., Iannielli, A., *et al*. (2016) The endoplasmic reticulum-mitochondria interface is perturbed in PARK2 knockout mice and patients with PARK2 mutations. *Hum. Mol. Genet.*, **25**, 2972–2984.
65. Lee, S., Sterky, F.H., Mourier, A., Terzioglu, M., Cullheim, S., Olson, L. and Larsson, N.G. (2012) Mitofusin 2 is necessary for striatal axonal projections of midbrain dopamine neurons. *Hum. Mol. Genet.*, **21**, 4827–4835.
66. Clark, J., Silvaggi, J.M., Kiselak, T., Zheng, K., Clore, E.L., Dai, Y., Bass, C.E. and Simon, D.K. (2012) Pgc-1alpha overexpression downregulates Pitx3 and increases susceptibility to MPTP toxicity associated with decreased Bdnf. *PLoS One*, **7**, e48925.
67. Goldberg, M.S., Fleming, S.M., Palacino, J.J., Cepeda, C., Lam, H.A., Bhatnagar, A., Meloni, E.G., Wu, N., Ackerson, L.C., Klapstein, G.J., *et al*. (2003) Parkin-deficient Mice Exhibit Nigrostriatal Deficits but Not Loss of Dopaminergic Neurons. *J. Biol. Chem.*, **278**, 43628–43635.
68. Gautier, C.A., Kitada, T. and Shen, J. (2008) Loss of PINK1 causes mitochondrial functional defects and increased sensitivity to oxidative stress. *Proc. Natl. Acad. Sci. U S A*, **105**, 11364–11369.
69. Perez, F.A. and Palmiter, R.D. (2005) Parkin-deficient mice are not a robust model of parkinsonism. *Proc. Natl. Acad. Sci. U S A*, **102**, 2174–2179.
70. Sterky, F.H., Lee, S., Wibom, R., Olson, L. and Larsson, N.G. (2011) Impaired mitochondrial transport and Parkin-independent degeneration of respiratory chain-deficient dopamine neurons in vivo. *Proc. Natl. Acad. Sci. U S A*, **108**, 12937–12942.
71. Pickrell, A.M., Huang, C.H., Kennedy, S.R., Ordureau, A., Sideris, D.P., Hoekstra, J.G., Harper, J.W. and Youle, R.J. (2015) Endogenous Parkin Preserves Dopaminergic Substantia Nigral Neurons following Mitochondrial DNA Mutagenic Stress. *Neuron*, **87**, 371–381.
72. Dusonchet, J., Bensadoun, J.C., Schneider, B.L. and Aebischer, P. (2009) Targeted overexpression of the parkin substrate Pael-R in the nigrostriatal system of adult rats to model Parkinson's disease. *Neurobiol. Dis.*, **35**, 32–41.
73. Sun, N., Yun, J., Liu, J., Malide, D., Liu, C., Rovira, I.I., Holmstrom, K.M., Fergusson, M.M., Yoo, Y.H., Combs, C.A., *et al*. (2015) Measuring In Vivo Mitophagy. *Mol. Cell*, **60**, 685–696.